Geometric and numerical techniques to compute conjugate and cut loci on Riemannian surfaces

Bernard Bonnard, Olivier Cots, Lionel Jassionnesse

Geometric and numerical techniques to compute conjugate and cut loci on Riemannian surfaces

Bernard Bonnard, Olivier Cots and Lionel Jassionnesse

Abstract We combine geometric and numerical techniques – the Hampath code – to compute conjugate and cut loci on Riemannian surfaces using three test bed examples: ellipsoids of revolution, general ellipsoids, and metrics with singularities on $\mathbf{S}^2$ associated to spin dynamics.

Key words: Conjugate and cut loci, optimal control, general ellipsoid, spin dynamics

1 Introduction

On a Riemannian manifold (M, g), the cut point along the geodesic γ emenating from q_0 is the first point where γ ceases to be minimizing, while the first conjugate point is where it ceases to be minimizing among the geodesics C^1-close to γ. Considering all the geodesics starting from q_0 they will form respectively the cut locus $C_{\text{cut}}(q_0)$ and the conjugate locus $C(q_0)$. The computations of the conjugate and cut loci on a Riemannian surface is an important problem in global geometry [1] and it can be extended to optimal control with many important applications [4]. Also convexity property of the injectivity domain of the exponential map is related to the continuity property of the Monge transport map T on the surfaces [6]. The structure of the conjugate and cut loci surfaces diffeomorphic to $\mathbf{S}^2$ was investigated in details

Bernard Bonnard
Institut de mathématiques de Bourgogne, 9 avenue Savary, 21078 Dijon, France, e-mail: bernard.bonnard@u-bourgogne.fr

Olivier Cots
INRIA, 2004 route des lucioles, F-06902 Sophia Antipolis, France, e-mail: olivier.cots@inria.fr

Lionel Jassionnesse
Institut de mathématiques de Bourgogne, 9 avenue Savary, 21078 Dijon, France, e-mail: lionel.jassionnesse@u-bourgogne.fr

by Poincaré and Myers [9], [10]. In the analytic case, the cut locus is a finite tree and the extremity of each branch is a cusp point. But the explicit computation of the number of branches and cusps points is a very complicated problem and only very recently was proved the four cusps Jacobi conjecture on ellipsoids [7], [12].

The aim of this article is to present techniques which led to the explicit computation of the cut and conjugate loci based on three examples, combining geometric techniques and numerical simulations using the Hampath code [5]. Geometry is used in a first step to choose appropriate coordinates to analyze the metric and the geodesics flow: curvature computation and principal lines of curvature. Also the explicit computations will be refered to the micro-local complexity of the Hamiltonian flow. This is clear in the example of an ellipsoid of revolution: geodesics can be meridians, the equator and a family of geodesics such that representing the metric in the normal form $g = \mathrm{d}\varphi^2 + m(\varphi)\mathrm{d}\theta^2$, θ increases or decreases monotonously while φ oscillates between φ^- and φ^+. The important task is to evaluate the first conjugate point t_{1c} which is solution to the Jacobi equation $\frac{\mathrm{d}^2 J}{\mathrm{d}t} + G(\gamma(t))J = 0$, where G is the Gauss curvature and such that $J(0) = J(t_{1c}) = 0$. Since in our case the usual Sturm theorem is not very helpful to estimate conjugate points, our approach is to estimate them in relation with the period mapping T of the φ-variable.

In the case of an ellipsoid of revolution it can be shown that conjugate and cut loci can be estimated with only the first and second order derivative of the period mapping [3].

The Hampath code is useful to analyze the geodesics and to evaluate conjugate points and the conjugate locus, using Jacobi fields and continuation method. In particular the analysis of the case of revolution can be easily extended to a general ellipsoid.

The time optimal transfer of three linearly coupled spins with Ising coupling described in [13] leads to study a one parameter Riemannian metric on $\mathbf{S}^2$ with equatorial singularity and which is a deformation of the Grushin case $g = \mathrm{d}\varphi^2 + \tan^2\varphi\mathrm{d}\theta^2$. Again the analysis of the flow and conjugate points computation led to describe the conjugate and cut loci for various values of the parameter.

2 Riemannian metrics on surfaces of revolution

We briefly recall the general tools to handle the analysis of surfaces of revolution with applications to the ellipsoids [3], [11].

2.1 Generalities

Taking a chart (U,q) the metric can be written in polar coordinates as

$$g = \mathrm{d}\varphi^2 + m(\varphi)\mathrm{d}\theta^2.$$

One use Hamiltonian formalism on T^*U, $\frac{\partial}{\partial p}$ is the vertical space, $\frac{\partial}{\partial q}$ is the horizontal space and $\alpha = p\mathrm{d}q$ is the (horizontal) Liouville form. The associated Hamiltonian is

$$H = \frac{1}{2}\left(p_\varphi^2 + \frac{p_\theta^2}{m(\varphi)}\right)$$

and we denote $\exp t\vec{H}$ the one-parameter group. Parameterizing by arc length amounts to fix the level set to $H = 1/2$. Extremal solutions of $\vec{H}$ are denoted $\gamma : t \to (q(t,q_0,p_0), p(t,q_0,p_0))$ and fixing q_0 it defines the exponential mapping $\exp_{q_0} : (t,p_0) \to q(t,q_0,p_0) = \Pi(\exp t\vec{H}(q_0,p_0))$ where $\Pi : (q,p) \to q$ is the standard projection. Extremals are solutions of the equations

$$\frac{\mathrm{d}\varphi}{\mathrm{d}t} = p_\varphi, \quad \frac{\mathrm{d}\theta}{\mathrm{d}t} = \frac{p_\theta}{m(\varphi)}, \quad \frac{\mathrm{d}p_\varphi}{\mathrm{d}t} = \frac{1}{2}p_\theta^2\frac{m'(\varphi)}{m^2(\varphi)}, \quad \frac{\mathrm{d}p_\theta}{\mathrm{d}t} = 0.$$

Definition 1. The relation $p_\theta = C^t$ is called **Clairaut** relation on surfaces of revolution. We have two types of specific solutions: **meridians** for which $p_\theta = 0$ and $\theta(t) = \theta_0$ and **parallels** for which $\frac{d\varphi}{dt}(0) = p_\varphi(0) = 0$ and $\varphi(t) = \varphi(0)$.

To analyze the extremal behaviours, we fix $H = \frac{1}{2}$ and we consider the mechanical system

$$\left(\frac{\mathrm{d}\varphi}{\mathrm{d}t}\right)^2 + V(\varphi, p_\theta) = 1$$

where $V(\varphi,p_\theta) = \frac{p_\theta^2}{m(\varphi)}$ is the **potential** mapping depending upon the parameter p_θ and parallels correspond to local extrema.

Assumptions 1 *In the sequel we shall assume the following*

- *(A1)* $\varphi = 0$ *is a parallel solution with a local minimum of the potential and the corrresponding parallel is called the* **equator**.
- *(A2) The metric is* **reflectionally symmetric** *with respect to the equator:* $m(-\varphi) = m(\varphi)$.

Micro-local behaviors of the extremals

We describe a set a solution confined to the segment $[-\varphi^{\mathbf{max}}, +\varphi^{\mathbf{max}}]$ where $\varphi^{\mathbf{max}}$ is the local maximum of V closest of 0. Such an extremal is such that φ oscillates periodically between $-\varphi^+$ and φ^+. The dynamics is described by:

$$\frac{\mathrm{d}\varphi}{\mathrm{d}t} = \pm\frac{1}{g}, \quad \frac{\mathrm{d}\theta}{\mathrm{d}t} = \frac{p_\theta}{m(\varphi)},$$

where

$$g(\varphi,p_\theta)=\sqrt{\frac{m(\varphi)}{m(\varphi)-p_\theta^2}}$$

and for an increasing branch one can parameterize θ by φ and we get

$$\frac{\mathrm{d}\theta}{\mathrm{d}\varphi}=\frac{g(\varphi,p_\theta)p_\theta}{m(\varphi)}=f(\varphi,p_\theta),$$

where

$$f(\varphi,p_\theta)=\frac{p_\theta}{\sqrt{m(\varphi)}\sqrt{m(\varphi)-p_\theta^2}}.$$

The trajectory $t\mapsto\varphi(t,p_\theta)$ is periodic and one can assume $\varphi(0)=0$. The period of oscillation T is given by

$$T=4\int_0^{\varphi^+}g(\varphi,p_\theta)\mathrm{d}\varphi$$

and the first return to the equator is at time $T/2$ and the variation of θ at this time is given by

$$\Delta\theta=2\int_0^{\varphi^+}f(\varphi,p_\theta)\mathrm{d}\varphi.$$

The mapping $p_\theta\in I\to T(p_\theta)$ is called the **period mapping** and $R:p_\theta\to\Delta\theta$ is called the **first return mapping**.

Definition 2. The extremal flow is called **tame** on I if the first return mapping R is such that $R'<0$.

Proposition 1. *For extremal curves with $p_\theta\in I$, in the tame case there exists no conjugate times on $(0,T/2)$.*

Proof. If $R'<0$, the extremal curves initiating from the equator with $p_\theta\in I$ are not intersecting before returning to the equator. As conjugate points are limits of intersecting extremals curves, conjugate points are not allowed before returning to the equator.

Assumptions 2 *In the tame case we assume the following*

(A3) At the equator the Gauss curvature $G=-\frac{1}{\sqrt{m(\varphi)}}\frac{\partial^2\sqrt{m(\varphi)}}{\partial\varphi^2}$ is positive and maximum.

Using Jacobi equation we deduce:

Lemma 1. *Under assumption (A3), the first conjugate point along the equator is at time $\pi/\sqrt{G(0)}$ and realizes the minimum distance to the cut locus $C_{\mathrm{cut}}(\theta(0)=0,\varphi(0)=0)$. It is a cusp point of the conjugate locus.*

Parameterization of the conjugate locus under assumptions (A1-2-3) for $p_\theta\in I$

Fixing a reference extremal γ, Jacobi equation is the variational equation:

$$\frac{\mathrm{d}\delta z}{\mathrm{d}t} = \frac{\partial \vec{H}(\gamma(t))}{\partial z}\delta z, \quad z = (q,p)$$

and a Jacobi field $J(t)$ is a non trivial solution of Jacobi equation. According to standard theory on surfaces, if γ is parametrized by arc length, $J_1(t) = (\delta q, \delta p)$ denotes the crucial Jacobi field vertical at time $t = 0$, that is $\delta q(0) = 0$ and such that $\langle p(0), \delta p(0)\rangle = 0$, that is restricting the Jacobi equation to $H = \frac{1}{2}$. Since $J_1(0)$ is vertical, $\alpha(J_1(0)) = 0$ and then $\alpha(J_1(t)) = 0$, and we have:

Proposition 2. *Conjugate points are given by the relation* $\mathrm{d}\Pi(J_1(t)) = 0$ *and*

$$\mathrm{d}\Pi(J_1(t)) = \left(\frac{\partial \varphi(t,p_\theta)}{\partial p_\theta}, \frac{\partial \theta(t,p_\theta)}{\partial p_\theta}\right).$$

In particular we have at any time the collinearity condition:

$$p_\varphi \frac{\partial \varphi}{\partial p_\theta} + p_\theta \frac{\partial \theta}{\partial p_\theta} = 0.$$

The conjugate locus will be computed by continuation, starting from the cusp point at the equator. Let $p_\theta \in I$ and $t \in (T/2, T/2+T/4)$. One has the formulae

$$\theta(t,p_\theta) = \Delta\theta(p_\theta) + \int_{T/2}^{t} \frac{p_\theta}{m(\varphi)}\mathrm{d}t$$

and on $[T/2,t]$, $\frac{\mathrm{d}\varphi}{\mathrm{d}t} < 0$, $\varphi < 0$. Hence

$$\int_{T/2}^{t} \frac{p_\theta}{m(\varphi)}\mathrm{d}t = \int_{\varphi(t,p_\theta)}^{0} f(\varphi,p_\theta)\mathrm{d}\varphi.$$

Using the collinearity condition, one has:

Lemma 2. *For* $p_\theta \in I$ *and conjugate times between* $(T/2, T/2+T/4)$ *the conjugate locus is solution of*

$$\frac{\partial \theta(\varphi,p_\theta)}{\partial p_\theta} = 0, \tag{1}$$

where $\theta(\varphi,p_\theta) = \Delta\theta(p_\theta) + \int_\varphi^0 f(\varphi,p_\theta)\mathrm{d}\varphi$.

This gives a simple relation to compute the conjugate locus by continuation. One notes $p_\theta \to \varphi_{1c}(p_\theta)$ the solution of eq. 1 initiating from the equator. Differentiating one has

$$\Delta\theta' + \int_\varphi^0 \frac{\partial f}{\partial p_\theta}\mathrm{d}\varphi = 0$$

at $\varphi_{1c}(p_\theta)$. Differentiating again we obtain

$$\Delta\theta'' + \int_{\varphi_{1c}}^0 \frac{\partial^2 f}{\partial p_\theta^2}\mathrm{d}\varphi - \frac{\partial \varphi_{1c}}{\partial p_\theta}\cdot\frac{\partial f}{\partial p_\theta} = 0.$$

One can easily check that $\frac{\partial f}{\partial p_\theta} > 0$ and $\frac{\partial^2 f}{\partial p_\theta^2} > 0$. In particular

$$\frac{\partial \varphi_{1c}}{\partial p_\theta} = \left(\Delta\theta'' + \int_{\varphi_{1c}}^{0} \frac{\partial^2 f}{\partial p_\theta^2} \mathrm{d}\varphi \right) \left(\frac{\partial f}{\partial p_\theta} \right)^{-1}.$$

and one deduces the following.

Proposition 3. *If $\Delta\theta'' > 0$ on I, then $\frac{\partial \varphi_{1c}}{\partial p_\theta} \neq 0$ and the curve $p_\theta \to (\varphi_{1c}(p_\theta), \theta_{1c}(p_\theta))$ is a curve defined for $p_\theta \in I$ and with no loop in the plane (φ, θ). In particular it is without cusp point.*

To simplify the computations we use the following lemma:

Lemma 3. *We have the relation*

$$R'(p_\theta) = \frac{T'(p_\theta)}{2p_\theta}.$$

2.2 Ellipsoids of revolution

The ellipsoid of revolution is generated by the curve

$$y = \sin\varphi,\ z = \varepsilon\cos\varphi$$

where $0 < \varepsilon < 1$ corresponds to the oblate (flattened) case while $\varepsilon > 1$ is the prolate (elongated) case. The restriction of the Euclidian metric is

$$g = F_1(\varphi)\mathrm{d}\varphi^2 + F_2(\varphi)\mathrm{d}\theta^2$$

where $F_1 = \cos^2\varphi + \varepsilon^2\sin^2\varphi$, $F_2 = \sin^2\varphi$. The metric can be written in the normal form setting:

$$\mathrm{d}\varphi = F_1^{1/2}(\varphi)\mathrm{d}\varphi.$$

Observe that φ oscillates periodically and θ is monotonous. Hence the period mapping can be computed in the (ψ, θ)-coordinate, $\psi = \pi/2 - \varphi$ and $\psi = 0$ is the equator. The Hamiltonian is

$$H = \frac{1}{2}\left(\frac{p_\varphi^2}{F_1(\varphi)} + \frac{p_\theta^2}{F_2(\varphi)} \right)$$

and with $H = 1/2$, one gets

$$\frac{\mathrm{d}\psi}{\mathrm{d}t} = \frac{(\cos^2\psi - p_\theta^2)^{1/2}}{\cos\psi(\sin^2\psi + \varepsilon^2\cos^2\psi)^{1/2}}.$$

Denoting $1-p_\theta^2=\sin^2\psi_1$ and making the rescaling $Y=\sin\psi_1 Z$, where $Y=\sin\psi$, one gets

$$\frac{(\varepsilon^2+Z^2\sin^2\psi_1^2(1-\varepsilon^2))^{1/2}}{(1-Z^2)^{1/2}}\mathrm{d}Z=\mathrm{d}t.$$

Hence the formulae for the period mapping is

$$\frac{T}{4}=\int_0^1\frac{(\varepsilon^2+Z^2\sin^2\psi_1(1-\varepsilon^2))^{1/2}}{(1-Z^2)^{1/2}}\mathrm{d}Z$$

which corresponds to an elliptic integral. The discussion is the following.

Oblate Case

In this case the Gauss curvature is increasing from the north pole to the equator and the problem is tame if the period mapping is such that

$$T'(p_\theta)<0<T''(p_\theta)$$

for each admissible $p_\theta>0$. The cut point of $q(0)=(\varphi(0),0)$ is given by $t_0(p_\theta)=T(p_\theta)/2$ and corresponds to the intersection of the two extremal curves associated to $\dot\varphi(0)$, and $-\dot\varphi(0)$. The cut locus $C_{\mathrm{cut}}(q(0))$ for not a pole is a segment of the antipodal parallel. If $q(0)$ is not a pole nor on the equator, the distance to the cut locus is the half-period of the extremal starting from $\varphi(0)$ with $\dot\varphi(0)=0$ and the injectivity radius is realized for $\varphi(0)=\pi/2$ on the equator, and is given by $\pi/\sqrt{G(\frac{\pi}{2})}$ where G is the Gauss curvature. The conjugate locus $C(q(0))$ of a point not a pole has exactly four cusps, two on the antipodal parallel which are the extremities of the cut locus segment and two on the antipodal meridian.

Prolate Case

In this case, the Gauss curvature is decreasing from the north pole to the equator and the first return mapping to the equator is an increasing function of $p_\theta\geq 0$. Given $q(0)=(\varphi(0),0)$ not on a meridian circle, the cut point $t_0(p_\theta)$ is given by solving $\theta(t_0,p_\theta)=\pi$ and corresponds to the intersection of the two extremal curves symmetric with respect to the meridian associated respectively to p_θ and $-p_\theta$. The cut locus of a point not a pole is a segment of the antipodal meridian. The conjugate locus $C(q(0))$ of a point not a pole has exactly four cusps, two on the antipodal meridian which are the extremities of the cut locus and two on the antipodal parallel.

Conclusion

To resume both cases are distinguished by the monotonicity property of the Gauss curvature or equivalently of the first return mapping. The cut loci are computed using the symmetric property of the extremal curves: in the oblate case, the symmetry of the metric with respect to the equator and in the prolate case the symmetry of the metric with respect to the meridian. Additionaly to this discrete symmetry, the symmetry of revolution ensures the existence of an additionnal one-dimensional group of symmetry which gives according to Noether theorem the first integral p_θ linear with respect to the adjoint vector and corresponds to a Clairaut metric.

3 General Ellipsoids

We shall extend the result on ellipsoids of revolution to general ellipsoids. Roughly spoken, the general case will mixed the oblate and the prolate case, which will be easily seen in the classification of the extremal flow.

3.1 Geometric Properties [7]

A general ellipsoid E is defined by the equation

$$\frac{x_1^2}{a_1}+\frac{x_2^2}{a_2}+\frac{x_3^2}{a_3}=1, \quad a_1>a_2>a_3>0$$

and we use the branched double covering parameterization of E $(\theta_1,\theta_2)\in T^2=S^1\times S^1\to E$:

$$\begin{aligned} x_1&=\sqrt{a_1}\cos\theta_1\sqrt{(1-\beta)\cos^2\theta_2+\sin^2\theta_2}\\ x_2&=\sqrt{a_2}\sin\theta_1\sin\theta_2\\ x_3&=\sqrt{a_3}\cos\theta_2\sqrt{\beta\cos^2\theta_1+\sin^2\theta_1} \end{aligned}$$

where $\beta=(a_2-a_3)/(a_1-a_3)\in(0,1)$ and the (θ_1,θ_2)-coordinates are related to the elliptic coordinates (λ_1,λ_2) by

$$\begin{aligned} \lambda_1&=a_1\sin^2\theta_1+a_2\cos^2\theta_1\\ \lambda_2&=a_2\cos^2\theta_2+a_3\sin^2\theta_2. \end{aligned}$$

In the coordinates (θ_1,θ_2) the restriction of the euclidian metric on $\mathbf{R}^3$ takes the form

$$g=(\lambda_1-\lambda_2)\left(\frac{\lambda_1}{\lambda_1-a_3}{\rm d}{\theta_1}^2+\frac{\lambda_2}{a_1-\lambda_2}{\rm d}{\theta_2}^2\right).$$

The metric has three main discrete symmetries defined for $i = 1,2$ by the following changes

$$\begin{array}{rcl} \theta_i & \longrightarrow & \pi - \theta_i, \\ \theta_i & \longrightarrow & -\theta_i. \end{array}$$

The associated Hamiltonian is

$$2H = \frac{1}{\lambda_1 - \lambda_2}\left(\frac{\lambda_1 - a_3}{\lambda_1} p_{\theta_1}^2 + \frac{a_1 - \lambda_2}{\lambda_2} p_{\theta_2}^2\right)$$

and an additional first integral quadratic in $(p_{\theta_1}, p_{\theta_2})$ is given by

$$F = \frac{1}{\lambda_1 - \lambda_2}\left(\frac{\lambda_1 - a_3}{\lambda_1}(a_2 - \lambda_2) p_{\theta_1}^2 - \frac{a_1 - \lambda_2}{\lambda_2}(\lambda_1 - a_2) p_{\theta_2}^2\right).$$

We have the following correspondences with the ellipsoid of revolution.

- In the limit case $a_1 = a_2 > a_3$ (oblate case), the metric g reduces to the form presented in 2.2 where $(\varphi, \theta) \equiv (\theta_1, \theta_2)$ and we have $F \geq 0$.
- In the limit case $a_1 > a_2 = a_3$ (prolate case), the metric g reduces to the form presented in 2.2 where $(\varphi, \theta) \equiv (\theta_2, \theta_1)$ and we have $F \leq 0$.

According to Liouville theory [2], the metric can be written in the normal form

$$g = (F_1(u_1) + F_2(u_2))\left(\mathrm{d}u_1^2 + \mathrm{d}u_2^2\right),$$

where u_1, u_2 are defined by the quadratures

$$\mathrm{d}u_1 = \sqrt{\frac{\lambda_1}{\lambda_1 - a_3}}\mathrm{d}\theta_1, \quad \mathrm{d}u_2 = \sqrt{\frac{\lambda_2}{a_1 - \lambda_2}}\mathrm{d}\theta_2$$

and see [8] for the relation with elliptic coordinates. The third fondamental form is given for $x_3 \neq 0$ by

$$III(\mathrm{d}x_1, \mathrm{d}x_2) = \frac{x_1 x_2 x_3}{a_1 a_2 a_3}\left(\frac{1}{a_3} - \frac{1}{a_1}\right)\mathrm{d}x_1^2 - \frac{x_1 x_2 x_3}{a_1 a_2 a_3}\left(\frac{1}{a_2} - \frac{1}{a_3}\right)\mathrm{d}x_2^2$$

$$+\frac{x_3}{a_3}\left(\left(\frac{1}{a_1} - \frac{1}{a_2}\right)\left(\frac{x_3}{a_3}\right)^2 - \left(\frac{1}{a_2} - \frac{1}{a_3}\right)\left(\frac{x_1}{a_1}\right)^2 - \left(\frac{1}{a_3} - \frac{1}{a_2}\right)\left(\frac{x_2}{a_2}\right)^2\right)\mathrm{d}x_1\mathrm{d}x_2$$

and we get the four umbilical points

$$\left(\pm\sqrt{a_1}\sqrt{1-\beta}, 0, \pm\sqrt{a_3}\beta\right)$$

which are $\{(0,0),(0,\pi),(\pi,0),(\pi,\pi)\}$ in (θ_1, θ_2)-coordinates. Besides in elliptic coordinates the lines $\lambda_i = \mathrm{Cst}$ are the curvature lines. Finally, taking the Liouville normal form, the Gauss curvature is given by

$$K(u_1,u_2)=\frac{F_1'(u_1)^2+F_2'(u_2)^2}{2\left(F_1(u_1)+F_2(u_2)\right)^3}-\frac{F''(u_1)+F''(u_2)}{2\left(F_1(u_1)+F_2(u_2)\right)^2}$$

or similarly, in the elliptic coordinates, one has

$$K(\lambda_1,\lambda_2)=\frac{a_1a_2a_3}{\lambda_1^2\lambda_2^2},\quad (\lambda_1,\lambda_2)\in[a_2,a_1]\times[a_3,a_2].$$

We give in Fig. 1 the Gauss curvature in the (θ_1,θ_2)-coordinates restricted to $(\theta_1,\theta_2)\in[0,\pi/2]\times[0,\pi/2]$ by symmetry. The maximum of K is at the intersection of the longest and the middle ellipses while the minimum is at the intersection of the shortest and the middle ellipses.

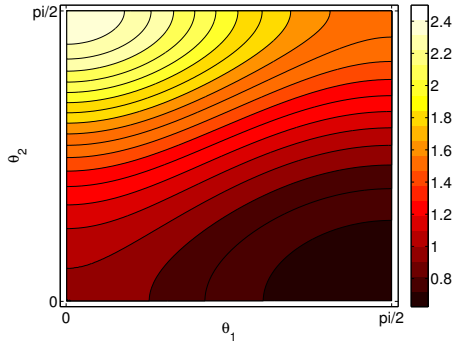

Fig. 1 Gauss curvature in (θ_1,θ_2)-coordinates for $(\theta_1,\theta_2)\in[0,\pi/2]\times[0,\pi/2]$. The maximum $a_1/(a_2a_3)$ is obtained at $(0,\pi/2)$ and the minimum $a_3/(a_2a_1)$ is at $(\pi/2,0)$.

3.2 Geodesic Flow

Parameterizing by arc length $H=\frac{1}{2}$ and setting $F=c$, the extremal equations are described by

$$\frac{\varepsilon_1\sqrt{\lambda_1}\mathrm{d}\theta_1}{\sqrt{\lambda_1-a_3}\sqrt{\lambda_1-a_2+c}}=\frac{\varepsilon_2\sqrt{\lambda_2}\mathrm{d}\theta_2}{\sqrt{a_1-\lambda_2}\sqrt{a_2-c-\lambda_2}}$$

and

$$\mathrm{d}t=\frac{\varepsilon_1\sqrt{\lambda_1}\sqrt{\lambda_1-a_2+c}}{\sqrt{\lambda_1-a_3}}\mathrm{d}\theta_1+\frac{\varepsilon_2\sqrt{\lambda_2}\sqrt{a_2-c-\lambda_2}}{\sqrt{a_1-\lambda_2}}\mathrm{d}\theta_2$$

where $\varepsilon_i=\pm1$ is the sign of $\mathrm{d}\theta_i/\mathrm{d}t$, $i=1,2$. The value c of F varies between $-(a_1-a_2)$ and (a_2-a_3) and the behavior of the extremals depends on the sign of c.

- If $0<c<a_2-a_3$, then $\theta_1(t)$ increases or decreases monotonously and $\theta_2(t)$ oscillates between $\nu_2(c)$ and $\pi-\nu_2(c)$, where $\nu_2(c)$ is defined by

$$\sin\nu_2(c)=\sqrt{\frac{c}{a_2-a_3}},\quad 0<\nu_2(c)<\frac{\pi}{2}.$$

These trajectories do not cross transversely the segments $\theta_2 = 0$ and $\theta_2 = \pi$ which degenerate into two poles in the oblate case. Here the longest ellipse $\theta_2 = \pi/2$ plays the role of the equator from the oblate case.

- If $-(a_1 - a_2) < c < 0$, then $\theta_2(t)$ increases or decreases monotonously and $\theta_1(t)$ oscillates periodically between $\nu_1(c)$ and $\pi - \nu_1(c)$ where $\nu_1(c)$ is defined by

$$\sin \nu_1(c) = \sqrt{\frac{-c}{a_1 - a_2}}, \quad 0 < \nu_1(c) < \frac{\pi}{2}.$$

These trajectories do not cross transversely the segments $\theta_1 = 0$ and $\theta_1 = \pi$ which degenerate into two poles in the prolate case. Here the longest ellipse plays the role of the meridian circle from the prolate case.

- The separating case $c = 0$ is the level set containing the umbilical points.

Arc length geodesic curves $\gamma(t) = (\theta_1(t), \theta_2(t))$ can be seen as a function of the parameter but we use the one from [7], introducing the unit tangent vector:

$$\nu(\eta) = \cos \eta e_1 + \sin \eta e_2$$

where (e_1, e_2) is the orthonormal basis

$$e_1 = \left(\frac{(\lambda_1 - \lambda_2)\lambda_1}{\lambda_1 - a_3} \right)^{-1/2} \frac{\partial}{\partial \theta_1}, \quad e_2 = \left(\frac{(\lambda_1 - \lambda_2)\lambda_2}{a_1 - \lambda_2} \right)^{-1/2} \frac{\partial}{\partial \theta_2}.$$

3.3 Results on the Conjugate and Cut Loci

According to [7] we have the following which generalized the case of an ellipsoid of revolution.

Proposition 4. *The cut locus of a non-umbilical point is a subarc of the curvature lines through its antipodal point and the conjugate locus has exactly four cusps.*

The Analysis

Fixing the initial point to $(\theta_1(0), \theta_2(0))$, the relation between η and c is given by:

$$c(\eta) = \big(a_2 - \lambda_2(\theta_2(0))\big) \cos^2 \eta - \big(\lambda_1(\theta_1(0)) - a_2\big) \sin^2 \eta$$

and let η_0 be the unique η such that $c(\eta_0) = 0$, $0 \leq \eta_0 \leq \frac{\pi}{2}$.

- The case $c > 0$, cf. Fig. 2. We use the parameterization (θ_1, θ_2) with $\theta_1 \in T^1$ and $0 \leq \theta_2 \leq \pi$.
  - For $\eta \in (0, \eta_0) \cup (\pi - \eta_0, \pi)$ the value of θ_2 along the geodesic increases until it reaches a maximum θ_2^+ and then it decreases. The cut time $t_0(\eta)$ is the **second** positive time such that θ_2 takes the value $\pi - s_2$.
  - For $\overline{\eta} = 2\pi - \eta$, the value of θ_2 along the geodesic decreases until it reaches a minimum θ_2^- and then it increases. The cut time $t_0(\overline{\eta})$ is the **first** positive time such that θ_2 takes the value $\pi - s_2$.
  - Besides, we have $t_0(\eta) = t_0(\overline{\eta})$ and $\gamma_\eta(t_0(\eta)) = \gamma_{\overline{\eta}}(t_0(\overline{\eta}))$.

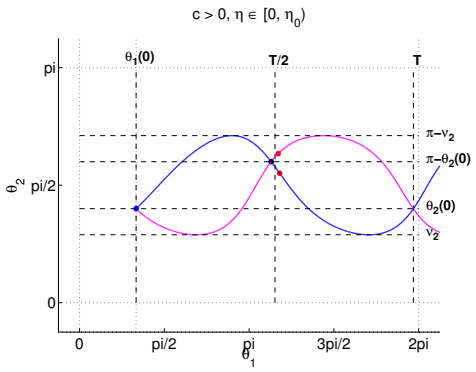

Fig. 2 Trajectories, cut and conjugate points in the case $c > 0$. The trajectory with $\dot{\theta}_2(0) > 0$ corresponds to $\eta \in (0, \eta_0)$ while the other corresponds to $\overline{\eta} = 2\pi - \eta$. The two conjugate points are plotted in red and come after the cut point in black. The period T of the θ_2-variable is equal for each trajectory and is represented with the half-period.

- The case $c \leq 0$, cf. Fig. 3. We use the parameterization (θ_1, θ_2) with $0 \leq \theta_1 \leq \pi$ and $\theta_2 \in T^1$.
  - For $\eta \in (\eta_0, \pi - \eta_0)$, θ_2 increases monotonously and let $t_0(\eta)$ be the first positive time t such that θ_2 takes the value $s_2 + \pi$. The cut time is given by $t_0(\eta)$.
  - For $\overline{\eta} = 2\pi - \eta$, θ_2 decreases monotonously and let $t_0(\eta)$ be the first positive time t such that θ_2 takes the value $s_2 - \pi$. The cut time is given by $t_0(\eta)$.
  - Besides, we have $t_0(\eta) = t_0(\overline{\eta})$ and $\theta_{1,\eta}(t_0(\eta)) = \theta_{1,\overline{\eta}}(t_0(\overline{\eta}))$.

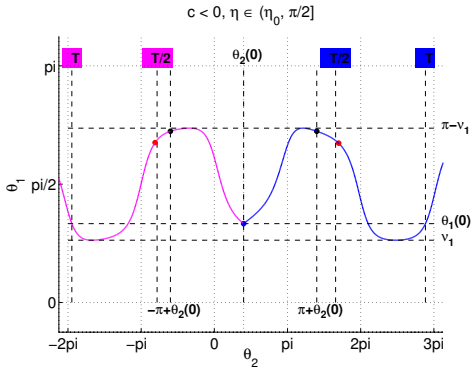

Fig. 3 Trajectories, cut and conjugate points in the case $c < 0$. The trajectory with $\dot{\theta}_2(0) > 0$ corresponds to $\eta \in (0, \eta_0)$ while the other corresponds to $\overline{\eta} = 2\pi - \eta$. The two conjugate points are plotted in red and come after the cut point in black. The periods of the θ_2-variable are not equal for each trajectory and are represented with the half-period.

Numerical Computation of Conjugate and Cut Loci

We fix the parameters of the ellipsoid $a_1 > a_2 > a_3 > 0$ such that $a_1 - a_2 \neq a_2 - a_3$ to avoid any additionnal symmetry. We take $(a_1, a_2, a_3) = (1.0, 0.8, 0.5)$ for the following computations. The initial point is $(\theta_1(0), \theta_2(0)) = (\pi/3, 2\pi/5)$ which gives generic results. Indeed, if the initial point is on $\theta_2 = 0$ or π, $c(\eta) \leq 0$ and there are only oblate-like extremals. Similarly, if $\theta_1(0) = 0$ or π, there are only prolate-like extremals. We present Figs. 4–7 the conjugate and cut loci.

One represents first the conjugate and cut loci on Fig. 4 using the double covering parameterization. We can distinguish the four cusps of the conjugate locus. Two of them on the horizontal line $\theta_2 = \pi - \theta_2(0)$ coming from the oblate-like extremals and the two others on the vertical line $\theta_1 = \pi - \theta_1(0)$ stemming from the prolate-like extremals. The cut locus is split into three parts, two on the line $\theta_2 = \pi - \theta_2(0)$ and one on $\theta_2 = \pi + \theta_2(0)$.

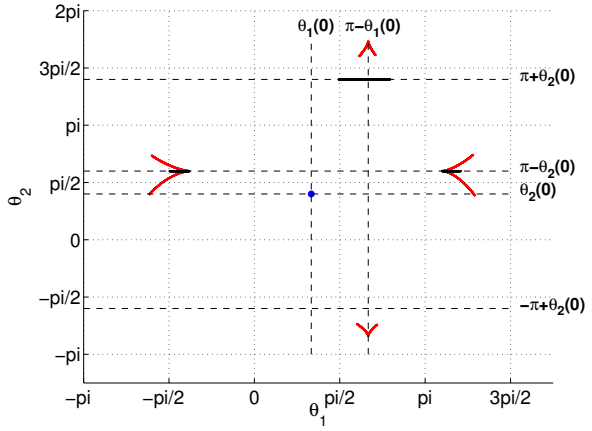

Fig. 4 Conjugate (in red dots) and cut (in black dots) loci, using the double covering parameterization. The initial point is marked with a blue dot.

One has some trajectories for various $\eta \in [0, 2\pi)$ with the cut and conjugate loci on Fig. 5 using again the double covering. One should notice that in red are plotted the four trajectories passing through the umbilical points with the parameterization (θ_1, θ_2) with $\theta_1 \in T^1$ and $0 \leq \theta_2 \leq \pi$. However, one could have used the second parameterization. These trajectories separate the oblate-like ($c > 0$) trajectories from the prolate-like ($c < 0$) ones. About the extremities of the three parts of the cut locus, two of them are coming from the trajectories γ_0 and γ_π for which the conjugate point and the cut point coincide. The two others extremities are located in the intersection of γ_{η_0} and $\gamma_{2\pi-\eta_0}$ and the intersection of $\gamma_{\pi-\eta_0}$ and $\gamma_{\pi+\eta_0}$, where $c(\eta_0) = 0$. The conjugate locus is revealed by the trajectories as we can see on the right subplot.

The conjugate and cut loci are given on the left subplot of Fig. 6 using the parameterization $(\theta_1, \theta_2) \in [0, 2\pi) \times [0, \pi]$ and on the right subplot of Fig. 6 in (x_1, x_2, x_3)-

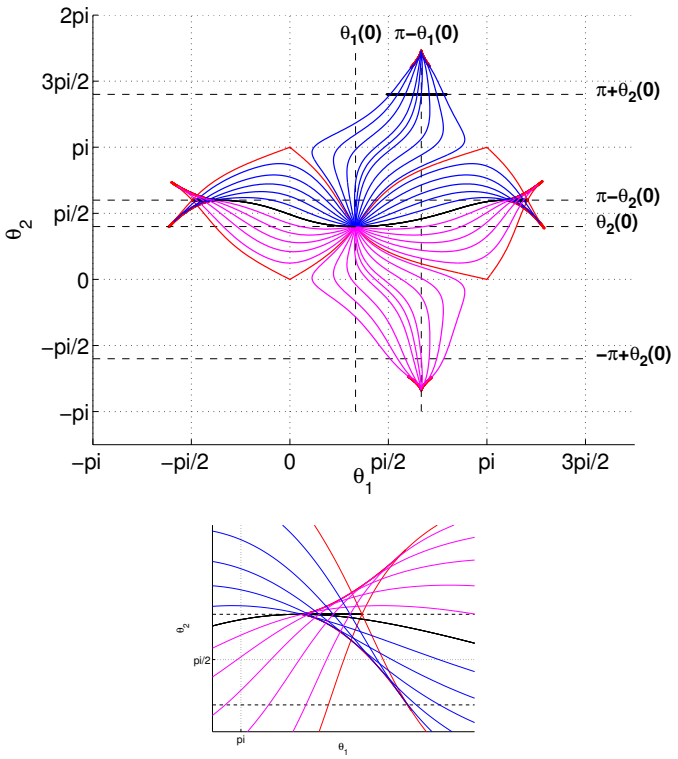

Fig. 5 (top) Various trajectories γ_η, $\eta \in [0,2\pi)$, with the conjugate (in red dots) and cut (in black dots) loci, using the double covering parameterization. (bottom) Zoom of the right-hand-side of the conjugate locus revealed by the trajectories. (both) For $\eta = 0$ or π, the trajectories are in black. They are tangential to the cut locus as we can see on the zoom. In blue are plotted the trajectories for $\eta \in (0,\pi)$ and in magenta for $\overline{\eta} = 2\pi - \eta$. The four trajectories in red such that $c(\eta) = 0$ pass through an umbilical point. They separate oblate-like behaviour from prolate-like one. The two intersections of these trajectories are junction of parts of the cut locus coming from oblate-like extremals and the cut locus coming from prolate-like extremals.

coordinates. To put together the four branches of the conjugate locus and the three segments of the cut locus, we first restrict θ_1 and θ_2 to $[0,2\pi)$ by modulo and then use a point reflection across (π,π) for points such that $\theta_2 \in [\pi,2\pi)$ for prolate-like extremals, as illustrated on the left subplot. The cut locus is a subarc of the curvature lines through its antipodal point, as expected, which extremities are cusps of the conjugate locus. The four branches of the conjugate locus does not have any symmetry in the generic case. However, if the initial point is on the longest and/or shortest ellipse, the conjugate locus has cusps on this ellipse and is symmetric with respect to it. In other words, if $\theta_2(0) = \pi/2$ then $t_1(\eta) = t_1(2\pi - \eta)$ and if $\theta_1(0) = \pi/2$ then $t_1(\eta) = t_1(\pi - \eta)$, where t_1 is the first conjugate time.

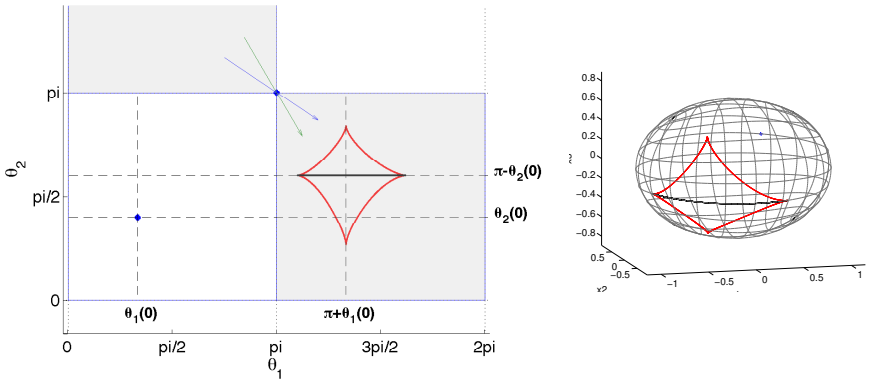

Fig. 6 Conjugate (in red dots) and cut (in black dots) loci, using the parameterization $(\theta_1,\theta_2) \in [0,2\pi) \times [0,\pi]$ for the left subplot and in (x_1,x_2,x_3)-coordinates for the right subplot. The initial point is marked with a blue dot. The two vectors crossing (π,π) illustrate the point reflection used to put together the different parts of the conjugate and cut loci.

Finally, the cut time t_0, the first conjugate time t_1 and the half-period $T/2$ of the oscillating variable is plotted Fig. 7. We can first notice that in the generic case, the half-period is not equal to the cut time, even for oblate-like trajctories. This is still true for an initial point on $\theta_1 = 0$ or π. The period is discontinuous when $c(\eta) = 0$ since the oscillating variable changes. The only one relevant symmetry is on the period mapping. Indeed, for η such that $c(\eta) > 0$, $T(\eta) = T(2\pi - \eta)$. The symmetry on t_1 being obvious.

Fig. 7 The cut time t_0, the first conjugate time t_1 and the half-period $T/2$ of the oscillating variable, with respect to the parameter $\eta \in [0,2\pi]$.

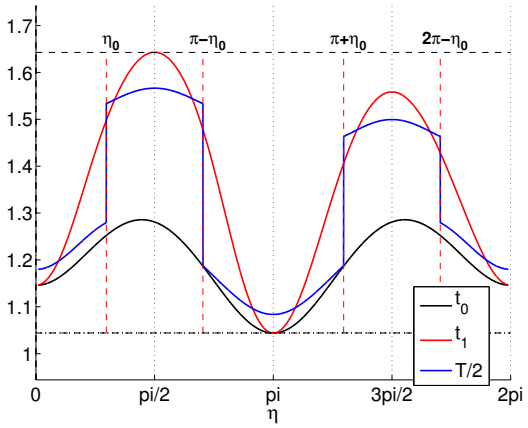

4 Dynamics of spin particles

The problem fully described in [13] arises in the case of a spin chain of three linearly coupled spins with Ising coupling and the problem is to transfer the state from the first spin to the third spin in minimum time. Using appropriate coordinates the dynamics takes the form:

$$\frac{\mathrm{d}}{\mathrm{d}t}\begin{pmatrix} r_1 \\ r_2 \\ r_3 \end{pmatrix} = \begin{pmatrix} 0 & -\cos\theta(t) & 0 \\ \cos\theta(t) & 0 & -k\sin\theta(t) \\ 0 & k\sin\theta(t) & 0 \end{pmatrix}\begin{pmatrix} r_1 \\ r_2 \\ r_3 \end{pmatrix}$$

where $k=1$ corresponds to equal coupling and the transfer is from $(1,0,0)$ to $(0,0,1)$. Setting $u_3=-\cos\theta$, $u_1=-k\sin\theta$, the dynamics is:

$$\dot r_1 = u_3 r_2, \quad \dot r_2 = -u_3 r_1 + u_1 r_3, \quad \dot r_3 = -u_1 r_2.$$

The minimum time problem is associated to the problem of transfering the system from $r_0=(1,0,0)$ to $r(T)=(0,0,1)$ and minimizing the functional:

$$\int_0^T \left(I_1 u_1^2 + I_3 u_3^2\right)\mathrm{d}t \longrightarrow \min.$$

We introduce the metric:

$$g = I_1 u_1^2 + I_3 u_2^2 = I_3\left(\frac{\mathrm{d}r_1^2 + I_1 I_3^{-1}\mathrm{d}r_3^2}{r_2^2}\right)$$

and this defines an almost Riemannian metric on the sphere $\mathbf{S}^2$:

$$g = \frac{\mathrm{d}r_1^2 + k^2\mathrm{d}r_3^2}{r_2^2}, \quad k^2 = \frac{I_1}{I_3}.$$

Lemma 4. *In the spherical coordinates $r_2=\cos\varphi$, $r_1=\sin\varphi\cos\theta$, $r_3=\sin\varphi\sin\theta$ the metric g takes the form*

$$g = (\cos^2\theta + k^2\sin^2\theta)\mathrm{d}\varphi^2 + \frac{(k^2-1)\sin 2\varphi\sin\theta\cos\theta\mathrm{d}\varphi\mathrm{d}\theta + \sin^2\varphi(\sin^2\theta + k^2\cos^2\theta)\mathrm{d}\theta^2}{\cos^2\varphi},$$

while the associated Hamiltonian function is given by

$$H = \frac{1}{4k^2\sin^2\varphi}\left(p_\varphi^2\sin^2\varphi(\sin^2\theta + k^2\cos^2\theta) + p_\theta^2\cos^2\varphi(\cos^2\theta + k^2\sin^2\theta) - 2\,(k^2-1)p_\varphi p_\theta\sin\varphi\cos\varphi\sin\theta\cos\theta\right).$$

We deduce the following

Lemma 5. *For $k = 1$*

$$H = \frac{1}{4}\left(p_\varphi^2 + p_\theta^2 \cot^2 \varphi\right),$$

and it corresponds to the so-called Grushin case $g = \mathrm{d}\varphi^2 + \tan^2 \varphi \mathrm{d}\theta^2$. The Grushin case is analyzed in details in [3]. We just remind that for each trajectory, θ increases or decreases monotonously while φ oscillates between φ^- and φ^+.

Moreover, we have

Lemma 6. *The family of metrics g depending upon the parameter k have a fixed singularity on the equator $\varphi = \pi/2$ and a discrete symmetry group defined by:*

- $H(\varphi, p_\varphi) = H(\pi - \varphi, -p_\varphi)$ *(reflexion with respect to the equator);*
- $H(\theta, p_\theta) = H(-\theta, -p_\theta)$ *(reflexion with respect to the meridian).*

Numerical Computation of Conjugate and Cut Loci

In what follows the conjugate and cut loci are computed for the fixed initial conditions: $\varphi(0) = \pi/2$, $\theta(0) = 0$, and are represented via the deformation of the parameter k starting from $k = 1$. There are two different cases to be analyzed: $k > 1$ and $k < 1$. Starting from the axis of symmetry, the Hamiltonian reduces to $H = p_\varphi^2/4$, and restricting the extremals to $H = 1$, we can parameterize the geodesics by $p_\varphi = \pm 2$, $p_\theta \in \mathbf{R}$. By symmetry we can fix $p_\varphi = -2$ and consider $p_\theta \geq 0$. For any k, the conjugate locus has a contact of order two at the initial point, as $p_\theta \to \infty$.

- $\mathbf{k \geq 1}$. We study the deformation of the conjugate and cut loci for $k \geq 1$ in Figs. 8–11. The key point is: when $k > 1$, θ is not monotonous for all the trajectories. This is true even for small k, like $k = 1.01$, taking $p_\theta = 0.1$ and $t_f > 14$.
  We denote $t_1(p_\theta, k)$ the first conjugate time and $q_1(p_\theta, k) = (\theta, \varphi)_{|t=t_1(p_\theta,k)}$ the associated conjugate point. In Fig. 8, we represent the map $k \in [1, 1.5] \mapsto q_1(k)$ for p_θ fixed to 10^{-4}. The value 1.5 is heuristically chosen to simplify the analysis. We can notice that $\theta(t_1(k))$ only takes approximately the values 0 and π and so it is on the same meridian as the initial point. It switches three times at $1 < k_1 < k_2 < k_3 < 1.5$, with $k_2 - k_1 \neq k_3 - k_2$. We then restrict the study of the conjugate locus to $k \leq k_3$ to simplify.

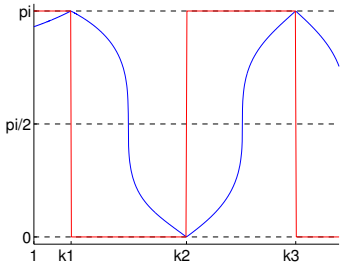

Fig. 8 The first conjugate point with respect to k, for p_θ fixed to 10^{-4}. In red is plotted $\theta(t_1(p_\theta, k))$ while we have in blue $\varphi(t_1(p_\theta, k))$. The θ-variable takes the values 0 and π. The values k_1, k_2, k_3 are approximately and respectively 1.061, 1.250, 1.429.

We can see in Fig. 9, three subplots which represent the deformation of one branch ($p_\varphi = -2$ and $p_\theta \geq 0$) of the conjugate locus resp. for k in $[1,k_1]$, $[k_1,k_2]$ and $[k_2,k_3]$. For any $k \in [1,k_3]$, the branch is located in the half-plane $\theta \geq 0$. If we denote $k_1 < \bar{k} < k_2$, the parameter value s.t. $\varphi(t_1(\bar{k})) = \pi/2$, then $\bar{k} \approx 1.155$ and the branch form a loop for $\bar{k} \leq k \leq k_3$.

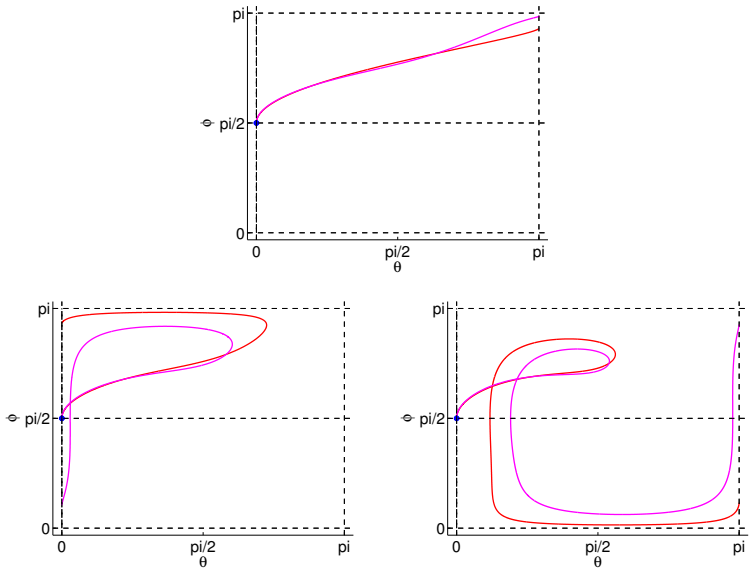

Fig. 9 The deformation of one branch ($p_\varphi = -2$ and $p_\theta \geq 0$) of the conjugate locus w.r.t. the parameter $k \in [1,k_3]$. (top) $k = 1.0$, 1.05. (left) $k = 1.1$, 1.2. (right) $k = 1.3$, 1.4.

The deformation of the conjugate locus can be explained analysing the behaviors of the trajectories. We describe four types of trajectories in (θ,φ)-coordinates (see Fig. 10), limiting the study to $k \leq k_3$ to simplify and $p_\theta \geq 0$ by symmetry. These trajectories clarify the evolution of the conjugate locus.

– The first type occuring for any k s.t. $1 \leq k \leq k_3$, is represented in the top left subplot of Fig. 10. Its characteristic is that the θ-variable is monotonous non-decreasing on $[0,t_1]$.

The three others trajectories do not have a monotonous θ-variable on $[0,t_1]$. We denote $\bar{t}$ the first time when the trajectory leaves the domain $0 \leq \theta \leq \pi$.

– The second type (top right) existing for $k_1 \leq k \leq k_3$ has no intersection on $[0,\bar{t}]$ and is such that $\theta(\bar{t}) = 0$.

The two last types of extremals have a self-intersection in the state-space in $[0,\bar{t}]$.

– The third kind of trajectories (bottom left) is such that $\theta(\bar{t}) = 0$ and is present for $\bar{k} \leq k \leq k_3$.
– The last one (bottom right) is only appearing for $k_2 \leq k \leq k_3$ and has $\theta(\bar{t}) = \pi$.

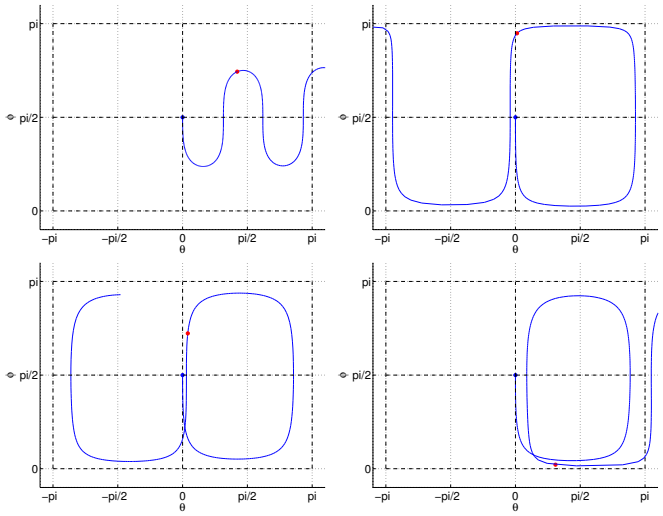

Fig. 10 The four types of trajectories which clarify the evolution of the conjugate locus. (top-left) existing for $1 \leq k \leq k_3$. (top-right) present for $k_1 \leq k \leq k_3$. (bottom-left) found for $\bar{k} \leq k \leq k_3$. (bottom-right) only for $k_2 \leq k \leq k_3$.

- $\mathbf{k \leq 1}$. The deformation of the conjugate locus in the case $k < 1$ is easier to interpret. We give on Fig. 11 the conjugate locus for $k \in \{0.8, 0.5, 0.2, 0.1\}$ with 15 chosen trajectories. The key point is the non-monotony of the θ-variable for $k < 1$.

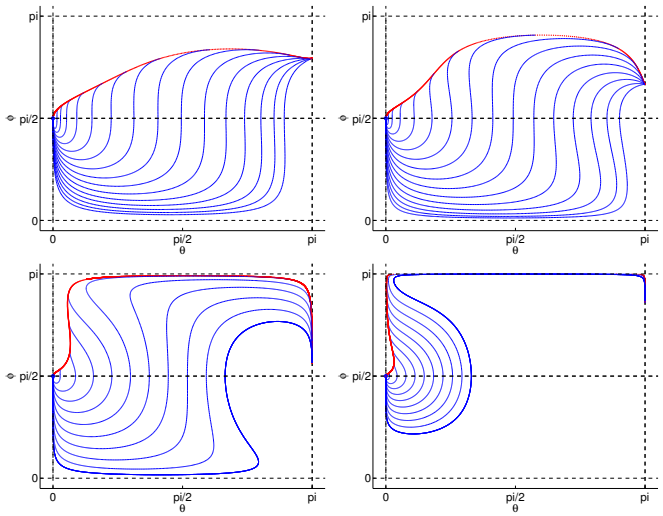

Fig. 11 Conjugate locus with 15 trajectories for $k = 0.8, 0.5, 0.2, 0.1$ from top left-hand to bottom right-hand.

We give a preliminary result about the cut loci to conclude these numerical computations. We denote $p_\theta > 0 \mapsto \Delta\theta_k(p_\theta) \in (0,\pi)$ the variation of θ at the first return to the equator (or first return mapping) as in §2.1. The previous numerical simulations suggest that $\Delta\theta_k$ is well defined for $k \in [0,k_3]$. The figure 12 suggests that for any k, the first return mapping is monotonous non-increasing and surjective. As a consequence, for a fixed k and starting from $\varphi(0) = \pi/2$, $\theta(0) = 0$, if there is no intersection between trajectories before the first return to the equator, then the cut locus is the equator minus the initial point. The figure 11 implies that there is no intersection before the first return to the equator for $k < 1$. Similar computations for $k \in [1,k_3]$ suggest the same.

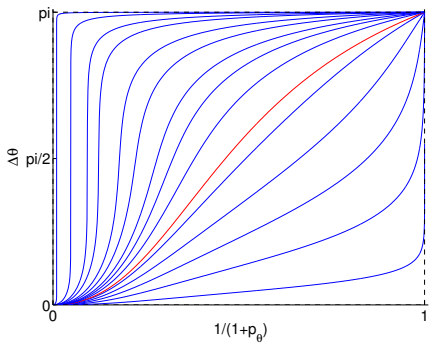

Fig. 12 First return mapping for different values of the parameter $k \in [0.1, 50]$. In red is plotted the curve for $k = 1$.

References

1. M. Berger, *A panoramic view of Riemannian geometry*, Springer-Verlag, Berlin (2003), xxiv+824.
2. A.V. Bolsinov and A.T. Fomenko, *Integrable geodesic flows on two-dimensional surfaces*, Monographs in Contemporary Mathematics, Consultants Bureau, New York (2000), xiv+322.
3. B. Bonnard, J.-B. Caillau, R. Sinclair and M. Tanaka, *Conjugate and cut loci of a two-sphere of revolution with application to optimal control*, Ann. Inst. H. Poincaré Anal. Non Linéaire, **26** (2009), no. 4, 1081–1098.
4. B. Bonnard and D. Sugny, *Optimal Control with Applications in Space and Quantum Dynamics*, vol. **5** of *Applied Mathematics*, AIMS, Springfield (2012), xvi+283.
5. J.-B. Caillau, O. Cots and J. Gergaud, *Differential continuation for regular optimal control problems*, Optimization Methods and Software, **27** (2011), no. 2, 177–196.
6. A. Figalli, L. Rifford and C. Villani, *Nearly round spheres look convex*, Amer. J. Math., **134** (2012), no. 1, 109–139.
7. J. Itoh and K. Kiyohara, *The cut loci and the conjugate loci on ellipsoids*, Manuscripta math., **114** (2004), no. 2, 247–264.
8. W. Klingenberg, *Riemannian geometry*, de Gruyter Studies in Mathematics, Berlin (1982), x+396.
9. S.B. Myers, *Connections between differential geometry and topology I. Simply connected surfaces*, Duke Math. J., **1** (1935), no. 3, 376–391.
10. H. Poincaré, *Sur les lignes géodésiques des surfaces convexes*, Trans. Amer. Math. Soc., **6** (1905), no. 3, 237–274.
11. K. Shiohama, T. Shioya and M. Tanaka, *The geometry of total curvature on complete open surfaces*, vol. **159** of *Cambridge Tracts in Mathematics*, Cambridge University Press, Cambridge (2003), x+284.
12. R. Sinclair and M. Tanaka, *Jacobi's last geometric statement extends to a wider class of Liouville surfaces*, Math. Comp., **75** (2006), no. 256, 1779–1808.
13. H. Yuan *Geometry, optimal control and quantum computing*, Phd Thesis, Harvard, (2006).